



Coupled Fluid-Kinetic Simulations of Dipolarization Fronts in Mercury's Nightside Magnetosphere



Alexander T. Cushen, ¹ Xianzhe Jia ¹, James Slavin ¹, Weijie Sun ²

¹University of Michigan, Department of Climate and Space Science and Engineering ²University of California, Berkeley, Space Sciences Laboratory

Mercury's Magnetosphere

Mercury has the most **similar magnetosphere to Earth**, as both are rocky planets with externally-driven dipole fields. However, they differ by:

- Weaker field ($\sim 1\%$ of Earth), resulting in ion gyroradius comparable to Mercury's radius
- Large conductive core and insulating crust instead of ionosphere
- Seasonally varying solar wind conditions with low Alfven Mach number which favors dayside reconnection

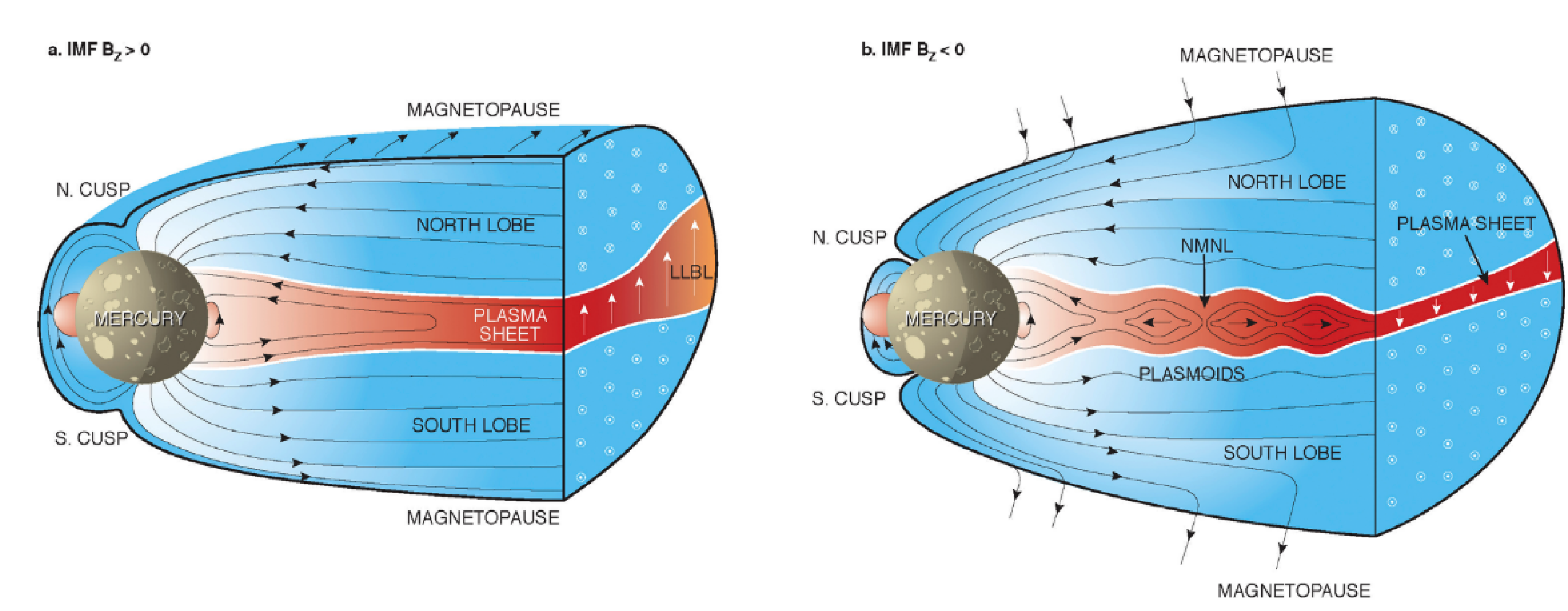


Figure 1. Magnetosphere under different solar wind (IMF) directions. From Slavin et al. 2012.

Southward IMF ($B_z < 0$) promotes substorms, where magnetic flux loads in the lobes. This flux is released through reconnection at Near Mercury Neutral Line (NMNL,) flowing planetward as a **dipolarization front** (Dewey et al. 2020).

Dipolarization fronts exhibit cross-tail asymmetry (Liu et al. 2019; Bard and Dorelli 2021), low density, and high flow speeds (Birn et al. 2011). They are generated in current sheet and propagate planetward, before slowing and diverting, generating cross-tail current:

$$j_{\perp} = \frac{\vec{B}}{B^2} \times \left(\rho \frac{d\vec{u}}{dt} + \nabla P \right)$$

Substorm current wedge is hypothesized to be created through inertial current term, and close through conductive core (Kepko et al. 2015).

MHD-AEPIC

MHD-AEPIC is a coupled fluid-kinetic simulation tool implemented through the Space Weather Modelling Framework. A global magnetohydrodynamic (MHD) solver evolves the magnetosphere, and adaptively embedded particle-in-cell (AEPIC) code models current sheet.

MHD: BATS-R-US solves single fluid equations on non-regular spherical mesh. Runs in steady-state mode to initialize domain, and then time-accurate for dipolarization front analysis. Hall physics (differential ion and electron motion) included to capture dayside reconnection.

PIC: FLEKS (Flexible Exascale Kinetic Simulator) evolves macroparticles through Cartesian grid to compute particle distribution function (Chen et al. 2023). Two-way couples to BATS-R-US at domain boundary.

Project Objectives

- Generation and propagation Under what solar wind conditions are dipolarization fronts generated?
- Substorm role How important are dipolarization fronts in particle and magnetic flux transport during a substorm?
- Planetary coupling Are dipolarizations front able to form a continuous substorm current wedge, and explain observations of low-altitude dipolarization regions?

Simulation Configuration

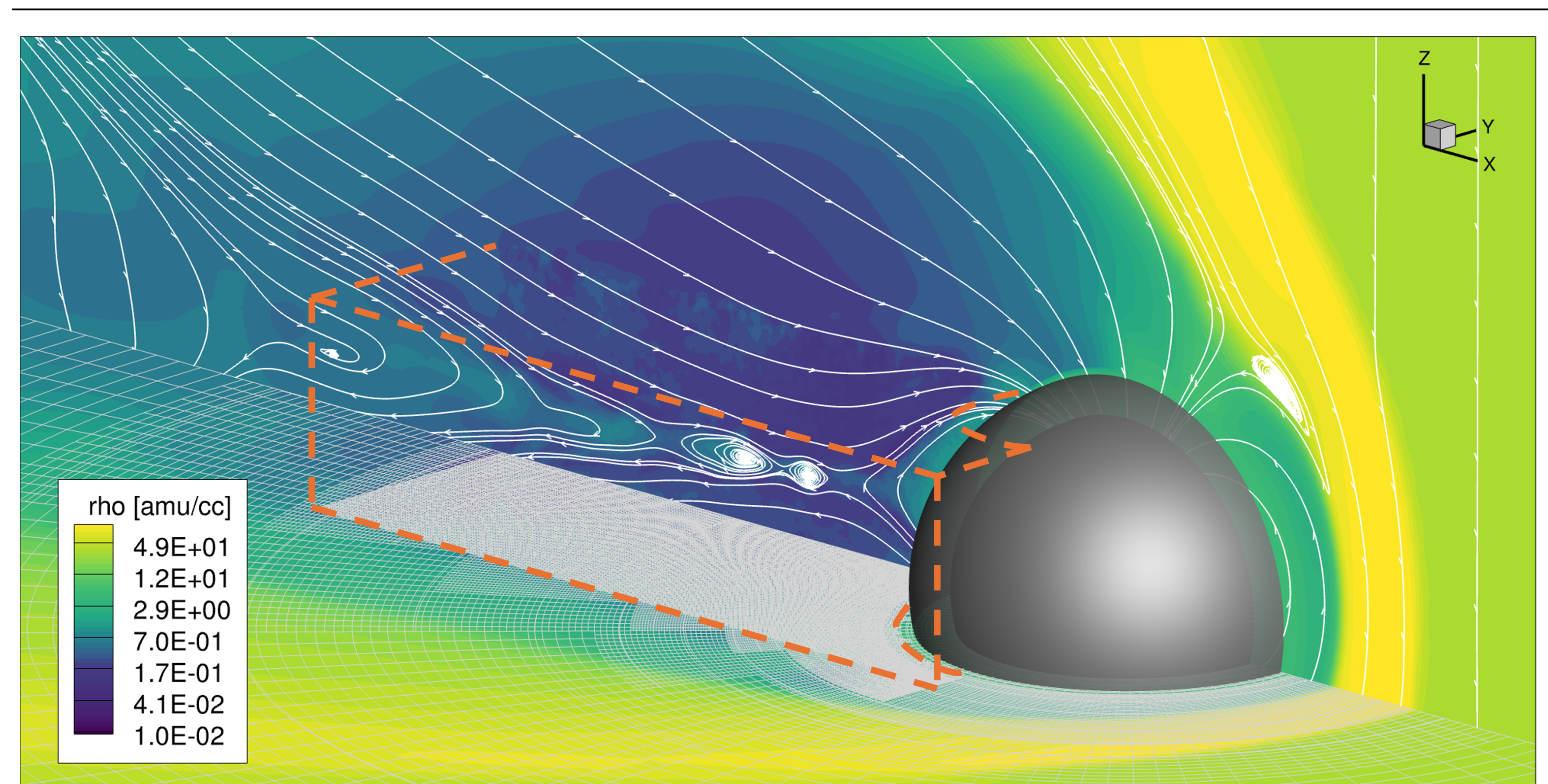
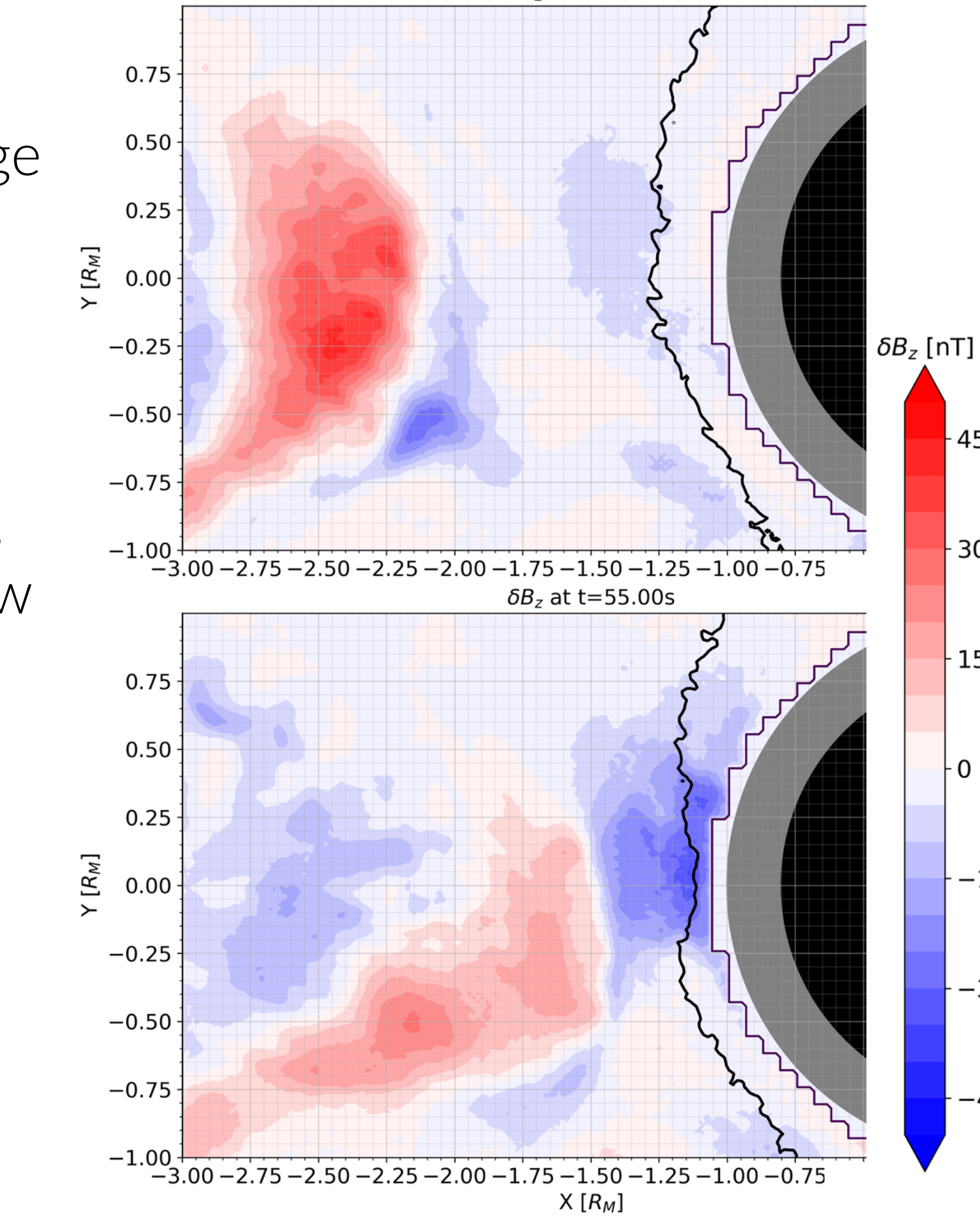


Figure 2. x-z and x-y slices of simulation domain; FLEKS region shown with orange border. Shading is plasma density. Magnetic field lines shown in white. Mesh grid shown in grey. Nominal run is 45 s FLEKS simulation, using 3×10^5 CPU hours on NASA Pleiades. Fluid data from FLEKS region saved at 0.05 s cadence. Idealised solar wind conditions chosen to drive substorm activity:

n [amu/cc]	T [K]	V _x [km/s]	B _z [nT]
36.0	87,000	-500	-23.0

Dipolarization Front Tracking

- 1. At each timestep, compute $\delta B_z = B_z \bar{B}_z$ where \bar{B}_z is average over t-5 to t-2 s.
- 2. Give a reference number to all clusters of cells of $\delta B_z > 5$ nT. Compare to previous time step to match clusters. If cluster has split, give the smaller child cluster a new reference number.
- 3. Compute cluster-averaged parameters like position, velocity, flux, and current.
- 4. Exclude any clusters with lifespan less than 2 s, or instantenous average plasma beta less than 1.



Flux Transport

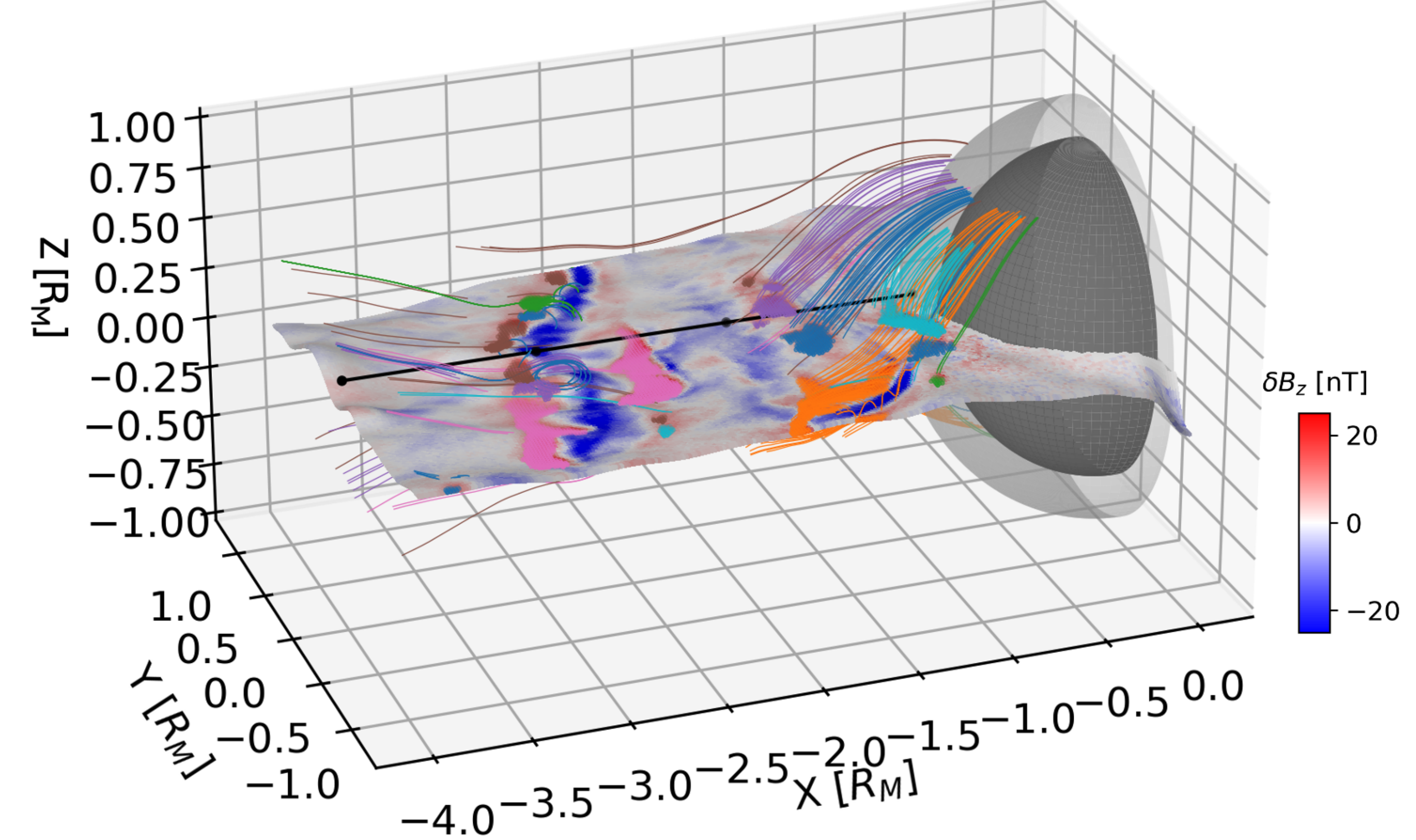


Figure 3. Colored regions correspond to identified DFs and their flux tubes. Current sheet, shaded by δB_z , extracted as smoothed surface of max plasma beta in FLEKS domain.

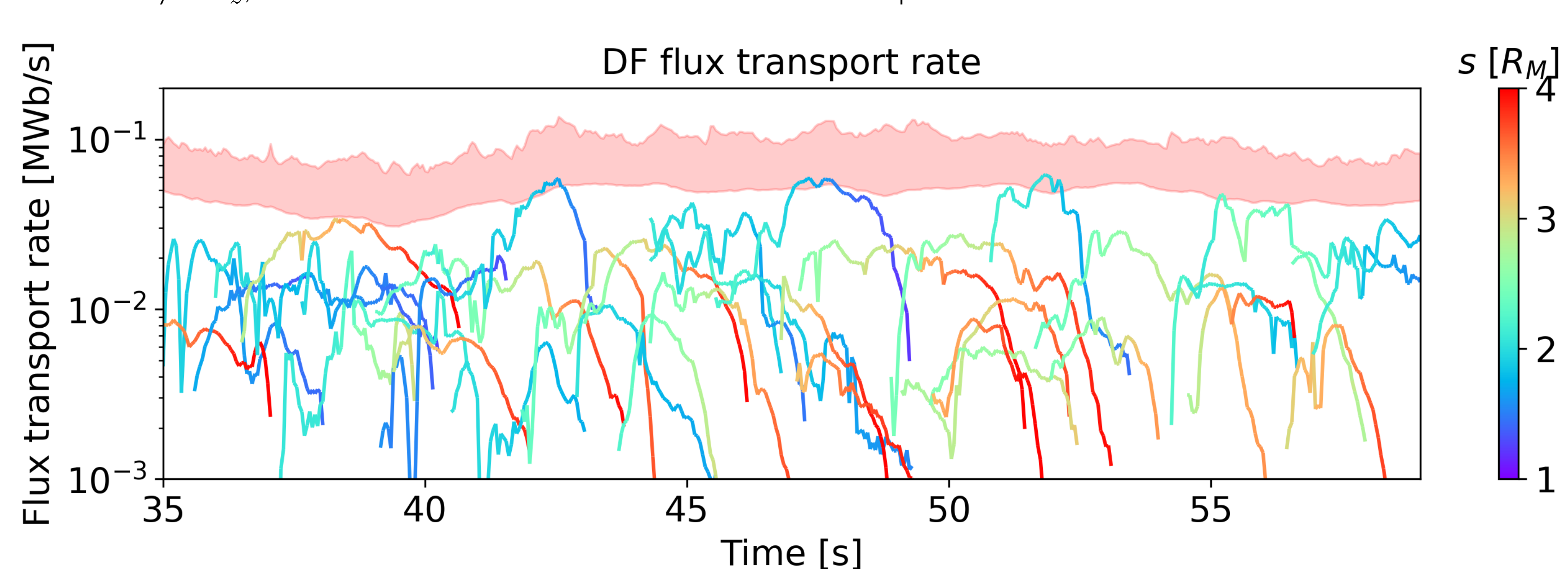


Figure 4. Red shaded region is total cross-tail flux transport rate. Lines are time-resolved transport rate for tracked DFs, and colored by distance to planet $s = \sqrt{X^2 + Y^2}$

Current signatures

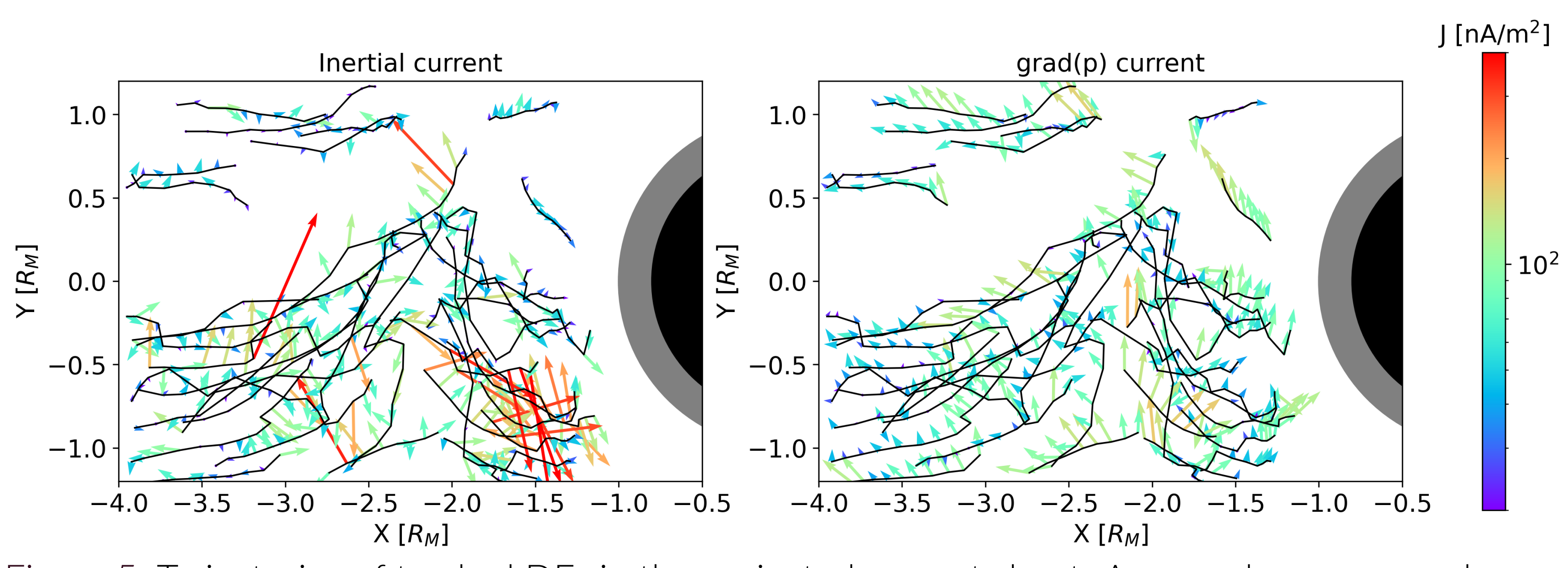


Figure 5. Trajectories of tracked DFs in the projected current sheet. Arrows show averaged inertial and pressure gradient current terms at 0.5 s cadence.

References

Bard, Christopher M. and John C. Dorelli (2021). "Magnetotail reconnection asymmetries in an ion-scale, Earth-like magnetosphere". In: Annales Geophysicae 39.6, pp. 991–1003. ISSN: 14320576. DOI: 10.5194/angeo-39-991-2021.

Birn, J. et al. (2011). "Bursty bulk flows and dipolarization in MHD simulations of magnetotail reconnection". In: Journal of Geophysical Research: Space Physics 116.1.

ISSN: 21699402. DOI: 10.1029/2010JA016083.

Chen, Yuxi et al. (2023). "FLEKS: A flexible particle-in-cell code for multi-scale plasma simulations". In: Computer Physics Communications 287, p. 108714. ISSN: 00104655. DOI: 10.1016/j.cpc.2023.108714. URL: https://doi.org/10.1016/j.cpc.2023.108714

00104655. DOI: 10.1016/j.cpc.2023.108714. URL: https://doi.org/10.1016/j.cpc.2023.108714.

Dewey, Ryan M. et al. (2020). "MESSENGER Observations of Flow Braking and Flux Pileup of Dipolarizations in Mercury's Magnetotail: Evidence for Current Wedge Formation". In: Journal of Geophysical Research: Space Physics 125.9, pp. 1–27. ISSN: 21699402. DOI: 10.1029/2020JA028112.

Kepko, Larry et al. (2015). "Substorm Current Wedge at Earth and Mercury". In: Magnetotails in the Solar System, pp. 361–372. DOI: 10.1002/9781118842324.ch21. Liu, Yi Hsin et al. (2019). "Three-Dimensional Magnetic Reconnection With a Spatially Confined X-Line Extent: Implications for Dipolarizing Flux Bundles and the

Dawn-Dusk Asymmetry". In: Journal of Geophysical Research: Space Physics 124.4, pp. 2819–2830. ISSN: 21699402. DOI: 10.1029/2019JA026539. Slavin, James A. et al. (2012). "MESSENGER and Mariner 10 flyby observations of magnetotail structure and dynamics at Mercury". In: Journal of Geophysical Research: Space Physics 117.1, pp. 1–17. ISSN: 21699402. DOI: 10.1029/2011JA016900.